Journal of Applied Polymer Science

Aging of polyamide 11. Part 2: General multiscale model of the hydrolytic degradation applied to predict the morphology evolution

Tobiasz Mazan,[1] Jens Kjær Jørgensen,[2] Andreas Echtermeyer[1]
[1]Department of Engineering Design and Materials, Norwegian University of Science and Technology, Trondheim 7034, Norway
[2]SINTEF Materials and Chemistry, Oslo 0373, Norway
Correspondence to: T. Mazan (E-mail: tobiasz.mazan@ntnu.no)

ABSTRACT: Accelerated aging tests are the conventional way to evaluate long-term degradation of polymers, in particular for offshore flexible risers. In this article, a multiscale model has been developed combining diffusion, chemical kinetic reactions, structure–property relationships, and composite models to provide faster and less labor extensive property predictions. A general methodology is presented and applied to predict the density and crystallinity evolution. Results are compared with experimental ageing of polyamide 11 in deoxygenated water at 120 °C. For both density and degree of crystallinity the modeled trend is close to the experimental test results. Accurate prediction of the morphological parameters during degradation allows extension of the multiscale model for the prediction of mechanical properties. © 2015 Wiley Periodicals, Inc. J. Appl. Polym. Sci. **2015**, *132*, 42630.

KEYWORDS: crystallization; degradation; oil & gas; polyamides; theory and modeling

Received 11 March 2015; accepted 18 June 2015
DOI: 10.1002/app.42630

INTRODUCTION

Polymeric materials find many applications in the offshore oil and gas industry with special emphasis on sealing and piping elements. In both cases unexpected failure can lead to significant economic and environmental hazards, which makes the understanding of long-term degradation mechanisms of key importance.[1] Absorption and diffusion of fluids, as well as the chemical reactions they can promote, are already well understood; nevertheless, the link between molecular effects and macroscopic material properties is still largely missing. Therefore, long term performance under chemical and mechanical factors is evaluated totally by long-term testing in the expected environment (typically a month to a year) and statistical extrapolation of the results to lifetimes of 20–50 years without understanding of science behind degradation phenomena.[2] This approach can serve industry pretty well under the assumption, that all degradation modes occurring in the material have been exposed in full prominence during test time. However, reality is often different and actual failure may happen long before (or after) the expected one.[3] Accelerated tests are often performed, but they require increased temperature and as such cannot be used for materials with a low melting point. Moreover both regular and accelerated tests are valid only for materials of a certain morphology exposed to a certain environment. Without understanding how each factor (and their interplay) affects global properties extrapolation of results to different cases is difficult. Very often even trace elements in an environment or slight differences in polymer microstructure can lead to significant changes in degradation over time.[4] Summarizing, currently used empirical–statistical approaches for predicting long term environmental degradation not only require very long testing times but also results, which can be obtained, are often far from being accurate.[2] Therefore, faster and more reliable evaluation methods are needed. The bottom-up multiscale approach is proposed here as a good way to address this problem. It is divided into four fundamental stages:

- Evaluation of the environmental agents (water, oxygen, acids, etc.) concentration profile in the polymer with time,
- Effect of chemical action of the environmental agent on the polymer molecular properties with time,
- Microstructure–property relationship yielding local mechanical properties of the polymer,
- Combining the local properties into global material properties.

This article as Part 2 of a series describes the details of the model and compares predictions against the morphology data: density and crystallinity. The experiments were shown in Part 1.[5] The model can also be expanded further to describe stiffness and strength. This aspect will be presented in Part 3.[6]

GENERAL MULTISCALE MODEL FOR DEGRADATION

There are numerous models concerning each separate stage of the presented method, however a holistic approach combining

them into a multiscale model has been missing. The aim of this work is to address this issue by developing a model linking chemical degradation on the microscale to macroscopic properties of the material. The approach is described first in general terms and then more specifically for Polyamide 11.

The general stages outlined here are shown in Figure 1. They will be applied for a specific case: the hydrolytic degradation of PA11. Two specific quantities will be addressed in the later parts of this article:

- Density
- Degree of crystallinity

Moreover the following properties will be considered in the succeeding paper:[6]

- Young's modulus
- Tensile strength
- Embrittlement threshold
- Mechanical equilibrium

The general approach suggested here for polymer properties prediction consists of four basic stages, as shown in Figure 1 and described in the following paragraphs.

Stage 1: Concentration Profile

The first stage is to calculate the concentration profile of the environmental agent in the selected material over time. To do so a certain diffusion model must be chosen and the model's constants need to be measured. Typically Fick's diffusion model is chosen, but if the shape of the concentration profiles is critical the validity of the model should be checked.

The concentration profile can be found by exploring literature resources or by performing tests on thin films. In the simplest case, diffusion parameters for different substances are treated as independent factors with possible model adjustment for their interplay. Basically two types of experiments are used to find both diffusivity and solubility of the material. In the first one, a flat plate (or thin film to safe time) is exposed on both sides to the solute and then the weight uptake as a function of time is recorded. There, initial rate of weight uptake is a function of diffusivity and terminal weight uptake is the solubility. In the other experiment, exposure is only one-sided and the amount of permeate going through the sample is measured.

Stage 2: Kinetic Model—Molecular Level

In the second stage, the local molecular structural changes with time are evaluated as a result of a certain concentration of reactive agent. This is a crucial part of the methodology as it predicts the molecular response in the long-term perspective, which cannot be encompassed empirically. The most important property changes addressed in this task are chemical (kinetic) reactions, swelling, and degree of crystallinity. A result of chemical reactions is typically chain scission resulting in a molecular weight decrease in the amorphous phase. For semicrystalline polymers, the molecular weight decrease is often followed by an increased ratio of crystalline phase, because the low molecular weight components can crystallize easily.[7] The most important

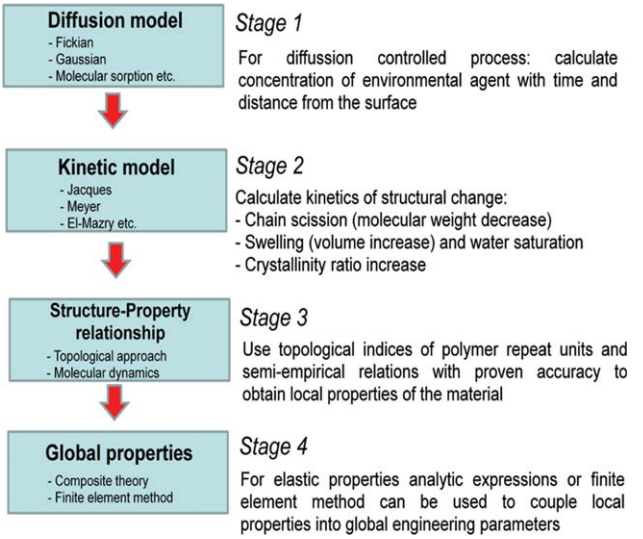

Figure 1. General scheme showing the stages of multiscale modeling of polymers. [Color figure can be viewed in the online issue, which is available at wileyonlinelibrary.com.]

reactions will have to be identified along with at least some respective rate constants and species concentrations. Then kinetics of the microstructural change can be expressed in terms of kinetics of individual reactions. This would often require solving adequate differential equation system.[8] If reactions occur very quickly time dependence can be skipped and experimental structural change can be used directly.

Scale Bridging: Stage 2 to Stage 3

Individual models are designed to operate on quantities in certain scale ranging from subatomic calculation to design of large engineering structures. Sometimes it is possible to directly use output parameters from smaller scale model as an input for larger scale models. Most of the time, however, a scale bridging procedure is needed to integrate single-scale models and create larger multiscale model.

In the case of the multiscale model of degradation proposed here only one scale bridging procedure must be used. The kinetic model in stage 2 provides molecular weight of the aged material, while formulas in stage 3 are functions of monomer topology and glass transition temperature.

Therefore, the dependence of the glass transition temperature on molecular weight $T_g(M_n)$ should be obtained.) $T_g(M_n)$ can be found by using the Fox and Flory equation:[9,10]

$$T_g(M_n) \approx T_g^{\infty} - 0.002715 \frac{(T_g^{\infty})^3}{M_n} \quad (1)$$

where T_g^{∞} is the hypothetical T_g for infinite molecular mass. T_g^{∞} is a material specific parameter and can be obtained by assuming an initial T_g for a specified M_n and solving the former equation.

Stage 3: Structure–Property Relationship

Topological Approach. In the third stage, local mechanical properties are to be evaluated as a result of structural changes in the polymer. To do so, we will mainly use topological

formalism using connectivity indices defined via graph theoretical concepts as its main descriptors. Topology is simply the pattern of interconnections between atoms in a polymer repeat unit and connectivity indices contain information on electronic configuration and coordination number for each one of them.[9] Correlating these parameters with experimental data enables to quantitatively predict polymer properties from given structural information. It is typically done by expressing fundamental material properties (volume occupied by the molecule, cohesive energy, etc.) as a function of topology and combining them into derived properties (such as density or elastic constants).[9] It has been shown, that all the additive properties can be expressed in terms of linear combinations of graph theoretical invariants, which constitutes a theoretical basis for the method.[11] The procedure is supported by many theoretical and semiempirical interrelations with proven accuracy, for example, dependence of glass transition temperature on molecular weight. Extensive databases containing such correlations are already available and can be expanded for new properties and polymers by performing experiments or group contribution calculations.[9] This procedure has proven its robustness for practical cases many times.[9]

The topological approach by Bicerano has been chosen as a model for structure–property relationship in the amorphous phase.[9] The crystalline phase is considered impenetrable for environmental agents and thus has constant properties during degradation.

Key Concepts of the Topological Method. Based on the literature a summary of the key concepts of the topological approach is given here:[9]

- Connectivity indices

  Connectivity indices describe the topology (connectivity) of the monomer. They include two categories—primary and aggregate connectivity indices.

  - Primary indices

    The simple atomic connectivity index δ-describes the number of non-hydrogen atoms to which a given non hydrogen atom is bonded

    The valence atomic connectivity index δ^V-gives information on details of the electronic configuration of each non-hydrogen atom:

$$\delta^V \equiv \frac{Z^V - N_H}{Z - Z^V - 1} \tag{2}$$

    where is Z^V is a number of valence electrons of an atom, N_H is the number of hydrogen atoms bonded to an atom and Z is the atomic number of the atom.

    Simple and valence bond connectivity indices β are the product of simple and valence atomic indices respectively on the vertices (i and j) defining a given bond:

$$\beta_{ij} = \delta_i * \delta_j \text{ and } \beta^V_{ij} = \delta^V_i * \delta^V_j \tag{3}$$

  - Aggregate indices

    Zeroth-order and first-order aggregate connectivity indices, X_0, X_0^V, X_1, X_1^V are summations of the reciprocal square roots of the primary connectivity indices over either vertices (atoms) or edges (bonds) of the monomer:

$$X_0 \equiv \sum_{\text{vertices}} \left(\frac{1}{\sqrt{\delta}}\right) \tag{4}$$

$$X_0^V \equiv \sum_{\text{vertices}} \left(\frac{1}{\sqrt{\delta^V}}\right) \tag{5}$$

$$X_1 \equiv \sum_{\text{edges}} \left(\frac{1}{\sqrt{\beta}}\right) \tag{6}$$

$$X_1^V \equiv \sum_{\text{edges}} \left(\frac{1}{\sqrt{\beta^V}}\right) \tag{7}$$

- Fundamental properties

  Fundamental properties are properties in the microscale, for example, van der Waals volume, cohesive energy, and so on. They are correlated with aggregate connectivity indices X, structural parameters (e.g., number of rotational degrees of freedom), and correction terms N (e.g., number of amide groups) as descriptors of the polymer repeat unit using an equation of the general form given below:

$$\begin{aligned}\text{Microscale property} = (\Sigma aX) + (\text{Structural Parameters}) \\ + (\text{Atomic and Group Correction Terms})\end{aligned} \tag{8}$$

  where a is a fit parameter.

  A wide range of such combinations with different connectivity indices, structural parameters, correction terms, and fit parameters was obtained by Bicerano[9] and the parameters giving the best fit to experimental or literature data were chosen to be included in his topological model.

- Derived properties

  Derived properties are properties in the macroscale, for example, density, solubility, modulus. They can be expressed in terms of combinations of fundamental properties and thus indirectly relate to the topology of the monomer. Correlations developed by Seitz for mechanical properties are of key importance.[9,12] It is a semiempirical approach in which experimental data is fitted with equations from thermodynamic and molecular theories.[12]

Alternative Methods. A number of alternative approaches may be used instead of the topological approach or as a supplement. Examples are the group contribution technique, experiments, and molecular dynamics. The group contribution technique provides quantitative structure–property relationships. This method considers contributions to a certain mechanical or thermodynamic property made by all chemical groups (such as —CH_2— or —OH) constituting the polymer repeat unit.[13] The main limitation of this technique is that a polymer property cannot be predicted if a value of a single group contribution cannot be estimated, which triggered development of the topological approach described above.[9]

Moreover, it is possible to use the experimental method, which would require preparation of samples with different molecular weights, densities, and phase ratios followed by mechanical testing. Such an experiment in conjunction with chemical modeling should allow formulating time dependent property profiles. Nevertheless, the usefulness of this approach is limited by the ability to control the microstructure of samples obtained, for

example, it is difficult to synthesize a set of samples differing in molecular weight with otherwise identical microstructure. Samples will always be varying in parameters like density, polydispersity, amount of contamination, and so on resulting in uncertainty regarding the exact effect of each structural feature.

Molecular dynamics is another method. It involves building a polymer structure model on an atomistic scale and performing subsequent computer simulations. This method can give interesting qualitative insights into the workings of polymer materials. However, due to time limitation and scale bridging issues, it should be probably treated as a last instance tool for the quantitative evaluation.[14–16] Currently available computational power provides simulations on atomic level for not more than several nanoseconds.[17] Also, coupling between atomistic level and mesoscale is specific to each system modeled and not straightforward.[15,16]

Stage 4: Global Properties

The global effect of the local material degradation needs to be found. Materials containing a number of volume elements with different properties can be treated as composites. Various methods, such as Finite Element Analysis or composites theory, for example, Halpin,[18] can be used to combine the varying properties into global engineering parameters.

MULTISCALE MODEL FOR HYDROLYTIC DEGRADATION OF POLYAMIDE 11

This section shows how the general multiscale approach can be applied to the case of Polyamide 11 degradation. Models operating on different scale-levels have been chosen for their demonstrated accuracy and ability to fit the multiscale model in a relatively straightforward manner—avoiding major scale bridging issues. While diffusion and structure–property models will be similar for most polymers and can be adjusted by using different input parameters, the kinetic model is specific to one process in one material. In our case it is hydrolytic chain scission in Polyamide 11.

Stage 1: Fast Saturation

In the case of PA11 exposed to water diffusion proceeds very fast and the environmental agent can be considered uniformly distributed within the material.[19] Diffusion in polyamides is also generally assumed to follow Fick's law.[20]

Figure 2 shows the modeled relative concentration of water with time in the centre of a 20-cm diameter PA11 element:

$$c_{\mathrm{rel}} = \frac{c(x,t)}{c_0} \tag{9}$$

where $c(x, t)$ is the concentration at time t and distance x from the surface, c_0 is the concentration at a boundary located at position $x = 0$. The diffusion coefficient of water in Polyamide 11 was found in the literature.[19] To estimate water concentration the 1D-Fick's law was used:[21]

$$c(x,t) = c_0 \,\mathrm{efrc}\left(\frac{x}{2\sqrt{Dt}}\right) \tag{10}$$

where erfc is the complementary error function approximated here by the first two terms of its Taylor series, $2\sqrt{Dt}$ is the diffusion length providing a measure of how far the concentration has propagated in the x-direction by diffusion in time t.

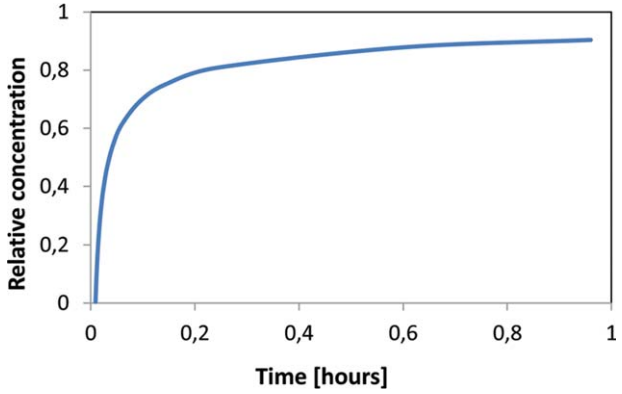

Figure 2. Modeled water concentration with time at distance $l/2 = 10$ cm from the surface, $D_{50\,^\circ\mathrm{C}} = 9.91 \times 10^{-9}$ cm^2/sec, Fickian behavior assumed. [Color figure can be viewed in the online issue, which is available at wileyonlinelibrary.com.]

It can be seen that after just 1 h exposure the relative concentration reaches 90%. It takes several days before complete saturation of the material.

For the remaining parts of the article, it will be assumed that diffusion of water into the PA happens very quickly compared to the typical lifetimes of 25 years or more required in offshore applications. The PA11 material will be seen as completely saturated and Stage 1 will not be considered any further.

Stage 2: Jacques Kinetic Model

Jacques model has been chosen to evaluate the kinetics of hydrolytic chain-scission due to its relative simplicity and confirmed accuracy.[22] A summary of this kinetic model is given in the following section.

The general governing reaction for PA11 hydrolysis is:[22]

$$\text{amide} + \text{water} \underset{k_R}{\overset{k_H}{\rightleftarrows}} \text{acid} + \text{amine} \tag{11}$$

The reaction occurs in amorphous phase only as the crystalline regions are considered impenetrable to water.[19]

The number of chain scissions (mol/kg) at time t can be expressed as follows:

$$n = \frac{1}{M_n} - \frac{1}{M_{n0}} \tag{12}$$

$$n = [\mathrm{Amide}]_0 - [\mathrm{Amide}] = [\mathrm{Acid}] - [\mathrm{Acid}]_0 = [\mathrm{Amine}] - [\mathrm{Amine}]_0 \tag{13}$$

where M_n is the number-average molar mass and the subscript zero corresponds to the initial (virgin) state. The basic kinetic equation can thus be written as:[22]

$$\begin{aligned} r(W) &= \frac{dn}{dt} = k_H[\mathrm{Amide}][\mathrm{Water}] - k_R[\mathrm{Acid}][\mathrm{Amine}] \\ &= k_H([\mathrm{Amide}]_0 - n)[\mathrm{Water}] - k_R([\mathrm{Acid}]_0 + n)([\mathrm{Amine}]_0 + n) \end{aligned} \tag{14}$$

where $r(W)$ is the rate of hydrolysis, k_H, k_R are the hydrolysis and recombination reaction constants.

Jacques model uses the following simplifications:[22]

Table I. Constants of Jacques Kinetic Model for Hydrolysis of PA11

Symbol	Name	Value	Unit
K_0	Rate constant at infinite temperature	7×10^{11}	1/day
E_k	$K(T)$ sensitivity factor ("activation energy")	97	kJ/mol
R	Universal gas constant	8.31	J/kg K
M_{ne0}	Equilibrium molecular weight at infinite temperature	2.36	kg/mol
E_m	$M_{ne}(T)$ sensitivity factor ("activation energy")	−6.46	kJ/mol
W_{s0}	water solubility at infinite temperature	1	mol/kg
E_w	$W_s(T)$ sensitivity factor ("activation energy")	4	kJ/mol
E_0	Initial amount of amide groups	5.46	mol/kg

- The amide conversion ratio at embrittlement is very small and can be neglected relatively to its initial concentration E_0
- Conditions of the polymerization process make initial acid concentration and initial amine concentration differ very little and are here assumed to be equal: $A_0 = B_0$

Experiments determined the quantities K (pseudo-rate constant) and M_{ne} (equilibrium molar mass) from which the basic rate constants k_R and k_H can be calculated:

$$k_R = \frac{KM_{ne}}{2} \quad \text{and} \quad k_H = \frac{k}{2M_{ne}[\text{Amide}]_0[\text{Water}]} \tag{15}$$

The temperature dependence of the rate constants (correlations for K and M_{ne}) and water solubility in the polymer is given by the Arrhenius law. Table I features all constants assumed in the Jacques model.[22]

Finally an expression for $M_n(t)$ is obtained by integrating eq. (14) and combining the result with eq. (12):[22]

$$M_n(t) = M_{ne}\frac{M_{n0}^{-1} + M_{ne}^{-1} + (M_{ne}^{-1} - M_{n0}^{-1})\exp(-Kt)}{M_{n0}^{-1} + M_{ne}^{-1} - (M_{ne}^{-1} - M_{n0}^{-1})\exp(-Kt)} \tag{16}$$

In this article, for the aging temperature $T = 120\,°C$ and initial molecular weight[5] $M_{n0} = 40.64$ kg/mol, values of the rate constants are as follows: $k_R = 0.77$ and k_H 0.0017 kg/mol day.

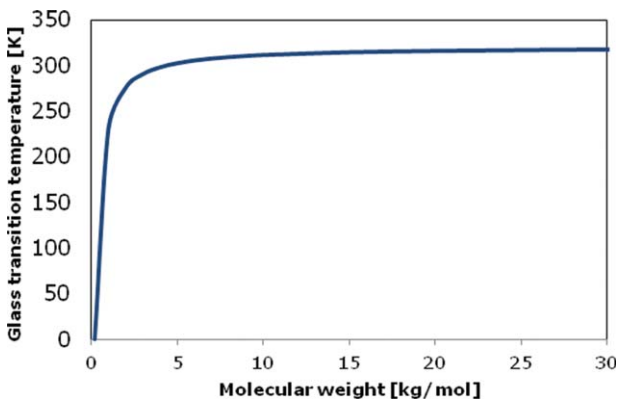

Figure 3. Glass transition temperature of amorphous PA11 as a function of molecular weight (Fox and Flory). [Color figure can be viewed in the online issue, which is available at wileyonlinelibrary.com.]

Scale Bridging: $T_g(M_n)$ Function

The Fox and Flory equation was used to obtain the $T_g(M_n)$ relationship as described previously. The result of this procedure for the studied PA11 sample (40.64 kg/mol[5], $T_g = 318$ K[23]) is shown in Figure 3. The glass transition temperature drops by 18 K for 5 kg/mol and falls rapidly when the molecular weight drops below about 3 kg/mol.

Stage 3: Structure–Property Relationship

The architecture of the PA11 repeat unit (as given in Figure 4) was analyzed with eqs. (2–7) and the following values for connectivity indices of PA11 were obtained to be used in the model:[9]

$$X_0 = 9.3555 \tag{17}$$

$$X_0^V = 8.4793 \tag{18}$$

$$X_1 = 6.3938, \tag{19}$$

$$X_1^V = 5.6612 \tag{20}$$

The exact procedure of obtaining structure–property relationships in the Stage 3 depends on property to be calculated. It is described in detail for density and crystallinity in later parts of this article and for the mechanical properties in the following paper.[6]

Stage 4: Uniform Properties

In this article describing PA11, we have an even distribution of water through the body, since the diffusion happens very quickly. Moreover the current modeling approach assumed the sample to be perfectly homogenous. This means properties will be the same throughout the material and global engineering properties do not need to be calculated. Therefore, Stage 4 will not be considered further.

PREDICTION OF THE PA11 MORPHOLOGICAL PROPERTIES

This section contains detailed property prediction procedures for the degree of crystallinity and density evolution. It also features a comparison between model and experiment. An

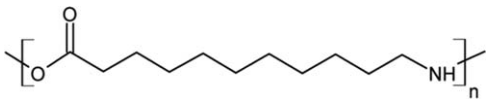

Figure 4. Molecular structure of the Polyamide 11 repeat unit. Empty vertices represent —CH_2 group.

Table II. Constituent Models of the Multiscale Approach to Predicting Density and Crystallinity

Property modeled (multiscale approach)	Constituent models
Density	Jacques[2]
	Fox and Flory[2-3]
	Bicerano[2-3] topological
	Crystallinity multiscale[3]
	Rule of mixtures[3]
Crystallinity	Jacques[2]
	Fox and Flory[2-2]
	Bicerano[2-2] topological
	Fayolle[2]

Numbers indicate stage or scale bridging in which certain model was introduced, reference in the main text.

analogous section in Part 3 of this article series will consider Young's modulus, yield strength, embrittlement, and mechanical equilibrium.[6]

Experimental results relevant for the modeling described here were reported in detail previously.[5] They are sometimes reported with error bars to give a statistically meaningful comparison between model predictions and laboratory testing. The error bars represent one standard deviation of parallel laboratory test results.

Input and Output Parameters

Table II lists the constituents of multiscale models applied here. Table III shows input parameters for these constituent models, their values to be used with PA11 property predictions along with reference and the output parameters produced by the model.

Input parameters can be generally divided into constants and variables. The constants are the parameters specific for a certain polymer system. The variables describe conditions specified by the application. Such variables include aging conditions (hydrolysis temperature and time) and initial parameters of the studied sample (initial molecular weight and degree of crystallinity).

The final output includes density and degree of crystallinity as functions of aging time as well as some intermediary parameters as listed in Table III.

Predicting Crystallinity

Chain scissions destroy the entanglement network in the amorphous phase and liberate small molecular segments which diffuse toward crystals surface and initiate chemicrystallisation.[7] The Fayolle model predicts the degree of crystallinity during degradation as a function of initial crystallinity, molecular weight and entanglement molecular weight.[7] To calculate

Table III. Input and Output Parameters of the Constituent Models in the Multiscale Approach

Model	Input parameters	Values chosen	Output parameters
Jacques	-T_{hyd}, hydrolysis temperature	120 °C—slightly above riser working conditions[23]	$M_n(t)$—number average molecular weight
	-M_{n0}, initial molecular weight	40.64 kg/mol—experiment[5] (part 1)	
	-t, hydrolysis time	Independent variable	
Fox and Flory	- T_g^{MW}, initial T_g for specified molecular weight	45 °C for 40.64 kg/mol, literature[23] T_g for M_{n0}	$T_g(M_n)$, glass transition temperature
	$M_n(t)$	Jacques model	
Bicerano topological	$T_g(M_n)$	Fox and Flory model	M_e, entanglement molecular mass; Φ_a, density of the amorphous phase
	Connectivity	$X_0 = 9.3555$, $X_0^V = 8.4793$, $X_1 = 6.3938$, $X_0^V = 5.6612$ from literature[9]	
	-M, monomer mass	174.2 g/mol from literature[9]	
	-l_m, monomer length	14.05 Å, self-calculated from geometry of monomer	
	-T, test temperature	25 °C, room temperature assumed	
Fayolle	-X_{c0}, initial crystallinity ratio	21.7%, experiment[5] (part 1)	-$X_c(t)$, degree of crystallinity
	M_{n0}, $M_n(t)$	Jacques model	
	M_e	Bicerano model	
Rule of mixtures (density)	- Φ_a, density of the amorphous phase	0.94 g/cm^3, Bicerano model	-$\Phi_{sc}(t)$, density of the semicrystalline polymer
	- Φ_c, density of the crystalline phase	1.25 g/cm^3, experiment[5] (part 1)	
	$X_c(t)$	Fayolle model	

crystallinity change during hydrolysis of PA11 molecular weight was taken from Jacques model and entanglement molecular weight was calculated from the topology of the monomer.

In the case of crystallinity prediction the topological approach operates on the level of the previously defined fundamental properties—essentially transforming one kinetic model—$M_n(t)$—Stage 2 (as defined in Figure 1) to another kinetic model $\chi(t)$—Stage 2b.

Calculation procedure of the degree of crystallinity is described below with indication of succeeding steps that must be taken. Only the first and last step belong to defined stages, while all the intermediate steps form the transformation procedure:

- Stage 2a: $M_n(t)$
  - Step 1. Molecular weight is obtained from Jacques kinetic model
- Horizontal transformation: topology to M_e
  - Step 2. Backbone rotational degrees of freedom are calculated from the number of single bonds and other structural features of the monomer:[9]

$$N_{\mathrm{BBrot}} = N_{\mathrm{BBbond}} + 0.5N_{\mathrm{FRbond1}} + 0.5N_{\mathrm{SFbond2}} \quad (21)$$

where N_{Bbond} is the number of single bonds in the backbone and not in a ring, N_{FRbond1} is the number of single bonds in the "floppy" ring in the backbone and N_{SFbond2} is the number of single bonds in the "semi-floppy" ring which is not directly bonded to any of the rigid rings

For PA11, we get $N_{\mathrm{BBrot}} = 12$

  - Step 3. Van der Waals volume V_w (cc/mol) is calculated as function of connectivity indices and correction terms:[9]

$$V_w = 2.28694\ X_0 + 17.14057\ X_1^V + 1.369231\ N_{vdW} \quad (22)$$

$$\begin{aligned} &N_{\mathrm{menobar}} + 0,5N_{\mathrm{mear}} + N_{\mathrm{alamid}} + N_{\mathrm{OH}} + 2N_{\mathrm{cyanide}} \\ &- 3N_{\mathrm{carbonate}} - 4N_{\mathrm{cyc}} - 2,5N_{\mathrm{fused}} + 2N_{\mathrm{C=C}} + 7N_{\mathrm{Si}} \\ &- 8N_{(-\mathrm{S}-)} - 4N_{\mathrm{Br}} \end{aligned} \quad (23)$$

where N_{menobar} is the number of methyl groups attached to nonaromatic atoms, N_{mear} is the number of methyl groups directly attached to atoms in aromatic rings, N_{alamid} is the total number of linkages between amide and similar (e.g., urea) groups and nonaromatic atoms, N_{OH} is the total number of —OH groups, N_{cyanide} is the number of —C≡N groups, $N_{\mathrm{carbonate}}$ is the number of (—OCOO—) groups, N_{cyc} is the number of nonaromatic rings with no double bonds along any of the edges of the ring, N_{fused} is the number of rings in "fused" ring structures, $N_{\mathrm{C=C}}$ is the number of carbon–carbon double bonds excluding those in ring structures. $N_{\mathrm{vdw}} = 1$ for PA11 (due to the amide bond present in the monomer) and $V_w = 185.4\,\mathrm{cm}^3/\mathrm{mol}$.

  - Step 4. Entanglement molecular weight M_e is calculated from the backbone rotational degrees of freedom, monomer mass, and length and connectivity indices.[9]

$$M_e \approx 1039.7 + 1.36411 * 10^{-23} \frac{N_{\mathrm{BBrot}} * M * V_w}{(l_m^3)}. \ [g/mol] \quad (24)$$

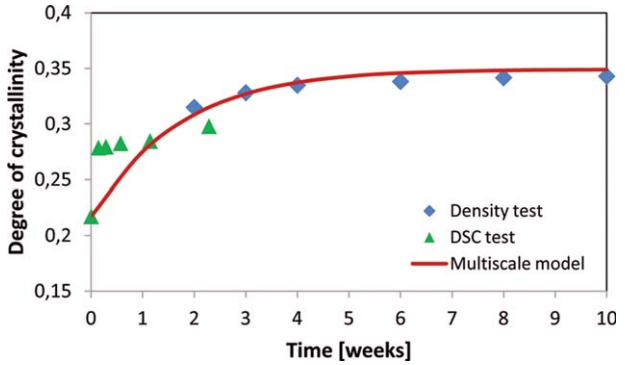

Figure 5. Comparison between modeled and experimental crystallinity evolution. [Color figure can be viewed in the online issue, which is available at wileyonlinelibrary.com.]

where M is the monomer mass (g/mol) and l_m is the monomer length in its fully extended conformation (cm).

The monomer weight of the PA11 is equal 174.2 g/mol. The monomer length l_m can be estimated from trigonometry of the polymer repeat unit or if possible by means of molecular modeling (e.g., Biosym's Polymer 6.0).[9] It has been found to be approximately equal to 14 Å for PA11. Finally for PA11 $M_e = 2.27$ kg/mol.

The expression for the entanglement molecular weight was obtained by fitting the rubber elasticity theoretical formula to group contribution data.[12]

- Stage 2b: $\chi(t)$
  - Step 5. The crystallinity ratio change is calculated as a function of initial crystallinity, molecular weight, and entanglement molecular weight (Fayolle model):[7]

$$\chi(t) = \chi_{c0} + \frac{1-\chi_{c0}}{\left[\left(\frac{M_{n0}}{M_e}\right)^{\frac{1}{2}} - 1\right]}\left[\left(\frac{M_{n0}}{M_n(t)}\right)^{\frac{1}{2}} - 1\right] \quad (25)$$

where χ_{c0} is the- initial crystallinity ratio, M_{n0} is the- initial molecular weight, M_n is the- number average molecular weight.

For our PA11 samples the initial crystallinity ratio was 21.7% and the initial molecular weight was 40.64 kg/mol—obtained from DSC test and viscosity measurements, respectively.[5]

Crystallinity Evolution

The degree of crystallinity was determined with DSC analysis for samples aged up to 2 weeks of exposure. For longer exposure times, crystallinity was calculated from density measurements.[5]

The comparison between modeled and experimental crystallinity evolution is featured in Figure 5. The prediction is fairly accurate for the DSC test and even very accurate for the density based evaluation. It gives an ultimate level of crystallinity:

$$\chi_\infty \approx 35\% \quad (26)$$

if started from initial level of 21.7%. This seems to be a perfect match with the experimental results.

Predicting Density

The density evolution of PA11 during degradation was calculated in five steps, starting with the densities of the amorphous and crystalline phases and crystallinity change $\chi(t)$ as obtained in the previous paragraph. The crystalline phase was assumed impenetrable to water thus with constant properties throughout hydrolytic degradation and its density was obtained experimentally. The density of the amorphous phase was calculated from $T_g(M_n)$ and the topology of the monomer using Seitz formulas for specific volume.[12] The specific volume occupied by the monomer is a structural parameter quantifying molecular packing arrangements.[9]

The steps of the density calculation procedure are described below together with the stages (see Figure 1), they belong to:

- Stage 2: $M_n(t)$ and $\chi(t)$
  - Step 1. The molecular weight is obtained from Jacques kinetic model, and the degree of crystallinity is taken from the multiscale crystallinity model
- Scale bridging: $M_n(t)$ to $V(t)$
  - Step 2. $T_g(M_n)$ is obtained as in Figure 3
  - Step 3. The specific volume $V(T)$ is calculated as a function of temperature, $T_g(M_n)$, connectivity indices and correction terms with one of three procedures, depending on test temperature T and $T_g(M_n)$ of the material:[9]

$$\text{For: } T \le T_g(M_n),\ \ T_g(M_n) > 298K:$$

$$\mathrm{V(T)} \approx \mathrm{V(298K)}\frac{1.42\ \ T_g(M_n)+0.15T}{1.42\ \ T_g(M_n)+44.7} \tag{27}$$

$$V(298K)=33.58596\ \ \mathrm{X_1^V}+26.518075\,N_{Si} \tag{28}$$

where N_{Si} features the number of silicon atoms in the monomer. N_{Si} is an atomic correction term, which are sometimes used to improve accuracy of correlations and has been found to correlate in general case with V (298 K).[9] However, it is irrelevant for PA11, which does not contain any silicon atoms.

$$\text{For}: T > T_g(M_n),\ \ T_g(M_n) > 298K:$$

$$\mathrm{V(T)} \approx \mathrm{V(298K)}\frac{1.57\ \ T_g(M_n)+0.3\left(T-T_g(M_n)\right)}{1.42\ \ T_g(M_n)+44.7} \tag{29}$$

$$\text{For}: T\ \ > T_g(M_n),\ \ T_g(M_n) \le 298K:$$

$$\mathrm{V(T)} \approx \mathrm{V(298K)}\ \ [1\ +\ \alpha_r(298K)(T-298)] \tag{30}$$

where α_r (298 K) is the coefficient of thermal expansion at room temperature:

$$\alpha_r(298K) \approx \frac{1}{298+4.23\ \ T_g(M_n),} \tag{31}$$

For the minor case of $T \le T_g(M_n),\ \ T_g(M_n) \le 298K$ there are no correlations with proven accuracy.[9]

The expressions for the specific volume were obtained from thermodynamic considerations.[9] For mechanical properties below the glass transition temperature the entropy was assumed to be constant, while above the glass transition temperature the material was assumed to behave as a rubber with a mostly entropic mechanical process.[12] Therefore, different expressions for $V(T)$ were obtained for glassy and rubbery polymers. Room temperature $T = 298$ K does not have any specific physical meaning with regard to properties; rather it is merely used as a reference temperature in the model.[9] The specific volume at a specified temperature was modeled as an extrapolation from the values of $V(T_g)$ and $V(298\ \mathrm{K})$.[12] For $T_g(M_n) \le 298$ K the interval between the two temperatures lies in the rubbery region. This forces inclusion of the two different coefficients of thermal expansion to cover the entire spectrum between the room temperature and 0 K. Therefore different expressions must be used in this case to calculate specific volume as well as density and mechanical properties depending on it.[9]

- Stage 3: $\Phi(t)$
  - Step 4. The density of the amorphous phase is calculated as a function of monomer weight and specific volume, crystalline density is taken as an input[5]

$$\varphi_a = \frac{M}{V(T)} \tag{32}$$

$$\varphi_c\ = 1.25\ \mathrm{g/cm^3}, \text{constant}$$

The monomer weight of the PA11 is equal 174.2 g/mol.

  - Step 5. Densities of the two phases and crystallinity evolution are combined to obtain density evolution

$$\varphi(t) = \varphi_c * \ \chi(t) + \ \varphi_a\ (1 - \ \chi(t)) \tag{33}$$

Density Evolution

Figure 6 shows modeled and measured density over the course of degradation. Experimental and modeled values tend to be very similar with a difference of about 1–2% for all aging times. The difference between modeled and experimental trend at shorter times can be explained by the effect of plasticizers. Plasticizers are present in new materials. When the PA11 is placed in water, the plasticizer gets leached out and is replaced by water.[5] This plasticizer–water interaction is rather complex and it is not accounted for in this model. After about 2 weeks the plasticizer extraction reached a plateau[5] and the model describes well the density change due to hydrolysis only. From that point onward density change nearly perfectly matches experimental results: the total density changes are controlled by the hydrolysis induced crystallinity increase, since the amorphous phase density hardly differs with aging time. Ideally, the testing should be repeated with non-plasticized material to clearly identify the effect of the plasticizer on the property changes.

DISCUSSION

The model proposed here for the prediction of morphological parameters is not only accurate but also particularly simple to use due to the analytic form of its expressions. Therefore, it can be easily programmed in languages such as MATLAB, calculated

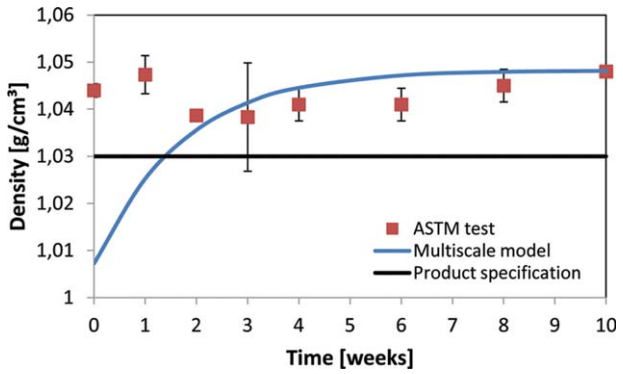

Figure 6. Comparison between modeled and experimental density evolution. [Color figure can be viewed in the online issue, which is available at wileyonlinelibrary.com.]

in Excel spreadsheets or even typed into a handheld calculator.[9] The predictive power of the model was demonstrated here in the case of PA11 hydrolytic degradation. The model can be applied to any other polymer providing that input parameters for diffusion and structure property models are known and a kinetic model for the specific chemical process in the specific material can be found. The latter somewhat limits the generality of the proposed approach. However, in practice, the kinetic models providing $M_n(t)$ as an output have been developed whenever it was required by industry.[24] Consequently such models exist for a wide range of practically important chain-scission processes in different materials.

Input parameters for the morphology evolution predictions can be obtained relatively easy. Data required for structure–property relationship of the amorphous phase (connectivity, mass, and length of the polymer repeat unit) can be directly calculated from the structure of the monomer. The density of the crystalline phase Φ_c and the glass transition temperature T_g are also material constants and can be found in the literature for many polymers.[9,23] Sample-dependent parameters such as initial molecular weight M_{n0} and initial degree of crystallinity χ_{c0} may also, in the first approach, be taken from the literature for a "typical sample" or ideally be obtained experimentally for the studied specimen. This can be done with viscometric[19] and spectrometric[25] measurements for M_{n0} or by XRD,[26] DSC,[5,7] FTIR,[7] and density[5,26] tests for. χ_{c0}. Among the mentioned parameters initial crystallinity appears to be the most difficult to find in the literature and may be available with good accuracy only for common polymers.

The proposed multiscale model allows obtaining property predictions based on the actual structure of the polymer and is therefore a step forward compared to simple and completely empirical extrapolation of the experimental tests results used today. This model is based on molecular processes although it is still a semiempirical approach, which relies heavily on correlations[9,12] to obtain properties in the amorphous phase. It is thus unable to provide any insights into actual mechanisms of the property emergence from a certain structure in the microscale. The model can however bring some insights into mechanisms in larger scales as will be discussed in the Part 3 of this study.[6]

Another limitation of the model is its conceptual simplicity. It considers only the most fundamental effects and in the case of morphology predictions provides only the degree of crystallinity ignoring parameters like crystallite size, shape, and orientation. For the calculation of both the density and crystallinity only average molecular mass is used and its distribution is neglected. It should be possible to develop the model further and address these effects in more detail. However, the good agreement with experiments shows that the simple approach taken here is sufficiently accurate for PA11.

The model does not include the effect of depleting plasticizer and therefore could not show this effect as observed during the first 2 weeks of aging for PA11. This is not seen as a severe limitation, because we are mostly interested in long-term predictions. However, when comparing density experimental data with the model, it is important to realize that results may deviate due to the effects of plasticizers. This is not a problem for crystallinity predictions as additive is not expected to have fundamental effect on the chemicrystalization process.

Generally the model should be understood as a practical tool aiding engineers with fast and accurate predictions of the morphology. The morphology predictions can be used further to predict global mechanical properties, such as Young's modulus and strength, as will be shown in Part 3 of this paper series.[6] This extension will provide some insight how the micromechanisms effect macroscopic properties of the semicrystalline polymer.

CONCLUSIONS

A general multiscale methodology for property predictions under aging is presented. Multiscale modeling results for the morphological properties of PA11 are compared with aging tests performed in water at 120 °C. A very good match between model and experiment is obtained for both the density and degree of crystallinity.

The model is easy to use, using simple semiempirical formulas, once the fundamental input parameters are obtained. The fundamental parameters can be found for most common polymers in the literature.

The effect of depletion of plasticizer and low molecular weight components is not modeled and needs to be evaluated separately. This effect is however irrelevant for crystallinity predictions and in the case of PA11 density may only be important in the first 2 weeks of exposure.

The successful prediction of PA11's structural parameters during degradation opens the possibility to predict engineering mechanical properties. An extension of the multiscale model will be presented in the succeeding paper (Part 3). The model provides a faster and less labor extensive engineering alternative to accelerated aging tests.

ACKNOWLEDGMENTS

This work is a part of the "PolyLife" project realized between SINTEF Materials and Chemistry, NTNU, PETROBRAS, ROSEN Group, Kongsberg Oil & Gas Technologies and FMC Technologies.

The authors would like to express their gratitude for the financial support by the Research Council of Norway (grant 193167). Randi Berggren performed accelerated aging and density measurements as part of her master thesis at NTNU.

REFERENCES

1. Teal, J. M.; Howarth, R. W. *Environ. Manag.* **1984**, *8*, 27.
2. Flynn, J. H. *J. Therm. Anal. Calorim.* **1995**, *44*, 499.
3. 4Subsea, PSA no. 0389-26583-U-0032, Revision 5: Unbonded Flexible Risers—Recent Field Experience and Actions for Increased Robustness; 4Subsea AS: Norway, **2013**.
4. Albertsson, A. C.; Barenstedt, C.; Karlsson, S. *J. Appl. Polym. Sci.* **1994**, *51*, 1097.
5. Mazan, T.; Berggren, R.; Jørgensen, J. K.; Echtermeyer, A. T. *J. Appl. Polym. Sci.* **2015**, *132*, 6249.
6. Mazan, T.; Jørgensen, J. K.; Echtermeyer, A. T. *J. Appl. Polym. Sci.* submitted.
7. El-Mazry, C.; Correc, O.; Colin, X. *Polym. Degrad. Stabil.* **2012**, *97*, 1049.
8. Devilliers, C.; Fayolle, B.; Laiarinandrasana, L.; Oberti, S.; Gaudichet-Maurin, E. *Polym. Degrad. Stabil.* **2011**, *96*, 1361.
9. Bicerano, J. Prediction of Polymer Properties; Marcel Dekker AG: New York, **2002**.
10. Flory, P. J. Principles of Polymer Chemistry; Cornell University Press: Ithaca, **1953**.
11. Gordon, M.; Temple, W. B. Chemical Applications of Graph Theory; Academic Press: New York, **1976**.
12. Seitz, J. T. *J. Appl. Polym. Sci.* **1993**, *49*, 1331.
13. van Krevelen, D. W. Properties of Polymers; Elsevier: Amsterdam, **1990**.
14. Fermeglia, M.; Pricl, S. *Progr. Org. Coat.* **2007**, *58*, 187.
15. Kremer, K.; Müller-Plathe, F. *Mol. Simul.* **2002**, *28*, 729.
16. Bouvard, J. L.; Ward, D. K.; Hossain, D.; Nouranian, S.; Marin, E. B.; Horstemeyer, M. F. *J. Eng. Mater. Technol.* **2009**, *131*, 041206.
17. Buehler, M. J. Atomistic Modeling of Materials Failure; Springer LLC: New York, **2008**.
18. Halpin, J. C.; Kardos, J. L. *J. Appl. Phys.* **1972**, *43*, 2235.
19. API Technical Report 17TR2, The Ageing of PA-11 in Flexible Pipes; API Publishing Services: Washington, DC, **2003**.
20. Wu, P.; Siesler, H. W. *Chem. Mater.* **2003**, *15*, 2752.
21. Bird, R. B.; Stewart, W. E.; Lightfoot, E. N. Transport Phenomena; Wiley: New York, **1976**.
22. Jacques, B.; Werth, M.; Merdas, I.; Thominette, F.; Verdu, J. *Polymer* **2002**, *43*, 6439.
23. Rilsan® PA11: Created From a Renewable Source; Arkema: France, **2012**.
24. Fayolle, B.; Richaud, E.; Colin, X.; Verdu, J. *J. Mater. Sci.* **2008**, *43*, 6999.
25. Domingos, E.; Pereira, T. M. C.; Filgueiras, P. R.; Bueno, M. I. M. S.; de Castro, E. V. R.; Guimarães, R. C. L.; de Sena, G. L.; Rocha, W. F. C.; Romão, W. *X-Ray Spectrom.* **2013**, *42*, 79.
26. Karacan, I. *Fibers Polym.* **2005**, *6*, 186.